ACS APPLIED MATERIALS & INTERFACES

Research Article

www.acsami.org

Uniform Microparticles with Controllable Highly Interconnected Hierarchical Porous Structures

Mao-Jie Zhang,[†] Wei Wang,*[,†] Xiu-Lan Yang,[†] Bing Ma,[†] Ying-Mei Liu,[†] Rui Xie,[†] Xiao-Jie Ju,[†] Zhuang Liu,[†] and Liang-Yin Chu*[,†,‡]

[†]School of Chemical Engineering, Sichuan University, Southern 1 Section, Yihuan Road, Chengdu, Sichuan 610065, P. R. China

[‡]State Key Laboratory of Polymer Materials Engineering, Sichuan University, Chengdu, Sichuan 610065, P. R. China

Supporting Information

ABSTRACT: A simple and versatile strategy is developed for one-step fabrication of uniform polymeric microparticles with controllable highly interconnected hierarchical porous structures. Monodisperse water-in-oil-in-water (W/O/W) emulsions, with methyl methacrylate, ethylene glycol dimethacrylate, and glycidyl methacrylate as the monomer-containing oil phase, are generated from microfluidics and used for constructing the microparticles. Due to the partially miscible property of oil/aqueous phases, the monodisperse W/O/W emulsions can deform into desired shapes depending on the packing structure of inner aqueous microdrops, and form aqueous nanodrops in the oil phase. The deformed W/O/W emulsions allow template syntheses of highly interconnected hierarchical porous microparticles with precisely and individually controlled pore size, porosity, functionality, and particle shape. The microparticles elaborately combine the advantages of enhanced mass transfer, large functional surface area, and flexibly tunable functionalities, providing an efficient strategy to physically and chemically achieve enhanced synergetic performances for extensive applications. This is demonstrated by using the microparticles for oil removal for water purification and protein adsorption for bioseparation. The method proposed in this study provides full versatility for fabrication of functional polymeric microparticles with controllable hierarchical porous structures for enhancing and even broadening their applications.

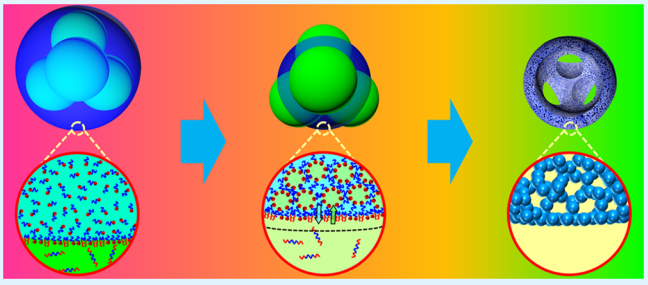

KEYWORDS: *emulsions, hierarchical structures, interfaces, microparticles, porous materials*

INTRODUCTION

With inspiration from hierarchical porous materials from nature such as biominerals, trabecular bones, and sea sponges, materials with hierarchical pores from nanometer to micrometer scales have been extensively developed for various applications.[1−3] Especially, porous polymeric materials in microparticle shape have attracted great interest in myriad fields, such as adsorption,[4,5] drug delivery,[6,7] tissue engineering,[8] sensing/detecting,[9,10] and chromatography.[11] Elaborate integration of controllable highly interconnected hierarchical porous structures containing micrometer-sized pores and nanometer-sized pores within polymeric microparticles enables combined advantages of pores at both micro- and nanoscales to achieve fascinating properties for enhanced applications. Usually, nanometer-sized pores with high interconnectivity and functionality can provide large functional surface area for interaction with molecules, while micrometer-sized pores can offer easier access with low resistance for the molecules, especially biomacromolecules, through the porous matrix. A combination of the nanometer-sized pores with micrometer-sized pores allows synergetic advantages of the large functional surface area and the enhanced mass transport to achieve advanced overall performance. Control of the porosities of both nanometer-sized pores and micrometer-sized pores plays an important role in determining the loading capacity and mass transfer profile. Meanwhile, the uniform size and shape of microparticles are crucial for regulating their assembly behaviors,[12,13] drug release kinetics,[14,15] and packing performance.[16−18] Therefore, development of uniform microparticles containing controllable highly interconnected hierarchical porous structures, with tunable pore size, porosity, functionality, and particle shape, is imperative for enhancing their broad applications.

Typically, pores in materials can be created by template-directed synthesis.[19] Pores with sizes ranging from nanometer-scale to micrometer-scale can be produced by templates such as assembled surfactants[20,21] or copolymers,[4,22−24] colloids,[25−29] emulsion drops,[30,31] bubbles,[32] phase-separated domains,[33] and bacterials.[34] Combination of multiple templating strategies enables production of hierarchical porous materials.[35−39] Manipulation of the macroscopic interfaces of the porous matrix can produce particle-shaped porous materials, but they

Received: February 3, 2015
Accepted: April 29, 2015
Published: April 29, 2015

DOI: 10.1021/acsami.5b01031
ACS Appl. Mater. Interfaces 2015, 7, 13758−13767

are usually particles with polydisperse sizes. With ultimate control of microdrop interfaces,[40,41] microfluidic techniques provide a powerful platform for engineering controllable porous polymer microparticles with monodisperse size. Most of the templating strategies can be adapted into the controllable microfluidic drops, with size ranging from several to hundreds of microns, for pore generation.[19] Thus, uniform porous polymeric microparticles can be fabricated by using monodisperse emulsion drops to shape the particle,[42] and using templates within the emulsions such as drops,[43,44] bubbles,[45] assembled copolymers,[46] as well as packed colloids,[10] to engineer the pores. However, these strategies that employ templates at one size scale usually produce porous polymeric microparticles containing pores with single size scale. Recently, hierarchical porous inorganic microparticles have been developed by assembly of silica nanoparticles on the inner drops of microfluidic W/O/W emulsions via evaporating the middle solvent layer.[47] The inner drops create micrometer-sized pores, while the voids between the packed silica nanoparticles create nanometer-sized pores in the inorganic microparticles; however, the nanoporosity remains difficult to flexibly adjust. Moreover, it requires post-treatment for further functionalization of these inorganic microparticles. Thus, for hierarchical porous polymeric microparticles, it is still challenging to simultaneously achieve accurate and independent control of their hierarchical porous structures with tunable pore size, porosity, functionality, as well as the particle shape in a single step. Therefore, techniques to realize such controls for developing controllable functional polymeric microparticles with highly interconnected hierarchical porous structures are highly desired.

Here we report a simple and versatile microfluidic approach for controllable fabrication of uniform polymeric microparticles containing highly interconnected hierarchical porous structures. The hierarchical porous microparticles possess well-defined micrometer-sized pores that are derived from the packed inner microdrops of W/O/W emulsions, and controllable nanometer-sized pores that are derived from water nanodrops formed in the oil phase of W/O/W emulsions via mass transfer. The pore size, porosity, functionality, and particle shape of the hierarchical porous microparticles can be individually and flexibly manipulated in one step. These microparticles elaborately combine the advantages of enhanced mass transfer, large functional surface area, and flexibly tunable functionalities from the hierarchical porous structures, thus providing an efficient strategy to physically and chemically achieve enhanced synergetic performances for extensive applications. This is demonstrated by applying the microparticles in oil removal for water purification and protein adsorption for bioseparation. The approach in this study provides full versatility for controllable fabrication of functional polymeric microparticles with highly interconnected hierarchical porous structures to achieve improved performances for myriad applications.

EXPERIMENTAL SECTION

Materials. Methyl methacrylate (MMA, ≥99%, Tianjin Bodi Chemicals), ethylene glycol dimethacrylate (EGDMA, 98%, Sigma-Aldrich), and glycidyl methacrylate (GMA, ≥97%, Sigma-Aldrich) were used as the oil phases of W/O/W emulsions for constructing the polymeric matrix of the microparticles. 2-Hydroxy-2-methyl-1-phenyl-1-propanone (HMPP, 97%, Sigma-Aldrich) was used as the oil-soluble photoinitiator. Polyglycerol polyricinoleate (PGPR) (99.8%, Danisco, Denmark) and poly(propylene oxide)-*block*-poly(ethylene oxide)-*block*-poly(propylene oxide) triblock copolymer Pluronic F127 (Bio-Reagent, Sigma-Aldrich) were used as emulsion stabilizers in the oil phase and the aqueous phase, respectively. Glycerin (≥99%, Chengdu Kelong Chemicals) was used to adjust the viscosity of the aqueous phase. Magnetic Fe_3O_4 nanoparticles (diameter: ~12 nm) modified with oleic acid for magnetic functionalization of the microparticles were prepared according to our previous work.[48] Fluorescein-isothiocyanate-labeled bovine serum albumin (FITC-BSA, Sigma-Aldrich) and bovine serum albumin (BSA, Sigma-Aldrich) were used for adsorption experiments. Other chemicals were all of analytical grade and used as received. Deionized water from a Milli-Q Plus water purification system (Millipore) was used throughout the experiments.

Fabrication of Hierarchical Porous Microparticles. The glass-capillary microfluidic device for generating W/O/W emulsions was fabricated according to our previous work.[49] The inner diameters of the injection tube, transition tube, and collection tube were 550, 150, and 300 μm, respectively. Typically, MMA (4 mL) containing cross-linker EGDMA (0.2 mL, 5% (v/v)), surfactant PGPR (0.2 g, 5% (w/v)), and photoinitiator HMPP (20 μL, 0.5% (v/v)) was used as the middle fluid. Deionized water (50 mL) containing glycerin (2.5 g, 5% (w/v)) and Pluronic F127 (0.5 g, 1% (w/v)) were used as the inner and outer aqueous fluids. Monodisperse W/O/W emulsions were generated by separately pumping the inner, middle, and outer fluids into the injection tube, transition tube, and collection tube of the microfluidic device. The generated emulsions were collected in a container and kept for 20 min to allow the mass-exchange between the oil phase and the aqueous phases for deformation of the W/O/W emulsions and formation of aqueous nanodrops in the oil phase. Then, the controllably deformed W/O/W emulsions were converted into hierarchical porous microparticles by UV-polymerization for 20 min. A 250 W UV lamp with an illuminance spectrum 250−450 nm was employed to produce UV light. The obtained microparticles were washed with ethanol and deionized water for further use.

For magnetic functionalization of the microparticles, 0.5% (w/v) magnetic nanoparticles were dispersed in the middle fluid by ultrasonic treatment. For fabrication of poly(EGDMA) (PEGDMA) microparticles, EGDMA solutions containing 0% (w/v), 5% (w/v), 10% (w/v), 20% (w/v), 30% (w/v), and 50% (w/v) of PGPR were used as the middle fluids. For fabrication of poly(MMA-*co*-EGDMA-*co*-GMA) microparticles, the oil phase containing GMA, MMA, EGDMA, and PGPR with volume ratio 25:25:50:10 was used as the middle fluid. For all the middle fluids, 0.5% (v/v) HMPP was added for UV-polymerization.

Morphological Characterization. The generation process of W/O/W emulsions in the microfluidic device was observed by high-speed digital camera (Phantom Miro3, Vision Research). The morphologies of W/O/W emulsions and microparticles were characterized by optical microscope (BX 61, Olympus) and field emission scanning electron microscope (FESEM, JSM-7500F, JEOL), respectively. The deformation processes of the W/O/W emulsions were monitored by the optical microscope. To estimate the deformation behavior, the oil shell thickness (δ) of W/O/W emulsions with a single inner microdrop, and the ellipticity (f) of W/O/W emulsions with two inner microdrops, were, respectively, calculated by the following equations:

$$\delta = (b - a)/2 \quad (1)$$

$$f = (b' - a')/b' \quad (2)$$

Here a and b are, respectively, the inner and outer diameters of the W/O/W emulsions with a single microdrop, and a' and b' are, respectively, the minor axis and major axis of the W/O/W emulsions with two microdrops.

The formation process of aqueous nanodrops in the oil phase was monitored by CLSM (SP5-II, Leica). EGDMA (ρ = 1.051 g cm^{-3}) microdrops containing 10% (w/v) PGPR, with density larger than water, were used as samples and added into aqueous phase for monitoring. Fluorescent Rhodamine B was dissolved in the aqueous phase to trace the diffused water in the oil microdrop during the formation of aqueous nanodrops.

Pore Characteristics and Mechanical Property. The sizes of the micrometer-sized pores were estimated by measuring the sizes of

DOI: 10.1021/acsami.5b01031
ACS Appl. Mater. Interfaces 2015, 7, 13758−13767

inner microdrop templates from the optical micrographs. The average pore sizes and specific surface areas of the nanoporous structures were determined by mercury intrusion porosimetry (PoreMaster 33, Quantachrome). Nanoporous PEGDMA microparticles and poly(MMA-*co*-EGDMA-*co*-GMA) microparticles, both prepared with 10% (w/v) PGPR, were used as the representative samples for measuring the sizes of the nanometer-sized pores. The effect of surfactant amount on the porosity of the nanoporous structures was studied by using PEGDMA microparticles prepared with 0% (w/v), 5% (w/v), 10% (w/v), 20% (w/v), 30% (w/v), and 50% (w/v) PGPR as samples. The porosity (ε) of the microparticles was calculated by the following equations:

$$\rho_0 = \frac{m_0}{V_0} \tag{3}$$

$$\rho_i = \frac{m_i}{V_i} \tag{4}$$

$$\varepsilon = 1 - \frac{\rho_i}{\rho_0} \tag{5}$$

Here ρ_0, m_0, and V_0 are, respectively, the density, mass quality, and volume of the nonporous microparticles without PGPR; and ρ_i, m_i, and V_i are the density, mass quality, and volume of the nanoporous microparticles with *i*% (w/v) (i = 5, 10, 20, 30, and 50) PGPR. For each type of microparticles, 500 dried samples were used for measurements of mass quality. The N_2 adsorption−desorption data of the microparticles were measured by using Quantachrome NOVA 1000e analyzer with N_2 adsorption at 77 K.

The mechanical strength upon compression of PEGDMA microparticles, which were prepared with the same size of ∼450 μm but different PGPR amounts, including 0% (w/v), 5% (w/v), 10% (w/v), 20% (w/v), 30% (w/v), and 50% (w/v), were investigated by using an electronic universal testing machine (EZ-LX, Shimadzu) at a speed of 0.1 mm/min.

Since hierarchical porous and nanoporous microparticles used as control groups for quantitative oil removal and BSA adsorption were prepared from emulsion templates with the same chemical compositions, the nanoporous matrixes possess the same porous property. Thus, the pore characteristics of nanoporous microparticles were characterized to reflect those of the nanoporous matrixes of hierarchical porous microparticles.

Oil Removal. EGDMA and benzyl benzoate were, respectively, used as model oils for oil removal. Briefly, the oil (30 μL) dyed with Lumogen Red 300 (LR300, BASF) was added into water and shaken into drops. Then, the magnetic hierarchical porous poly(MMA-*co*-EGDMA) microparticles containing three micrometer-sized pores were added into the water and mixed with the oil drops by shaking for oil adsorption. After that, the oil-adsorbed microparticles were separated by a magnet, and washed with ethanol for reuse.

The effect of hierarchical porous structure on the oil-adsorbing property was investigated by using poly(MMA-*co*-EGDMA-*co*-GMA) microparticles with nanoporous structures and different hierarchical porous structures for quantitative oil removal. The nanoporous structures of the samples were all fabricated with addition of 10% (w/v) PGPR in the recipe. For each type of samples, microparticles with total mass quality of 0.02 g were used. LR300-dyed EGDMA drops were gradually added (5 μL per time) into water that contained the sample microparticles for oil removal.

BSA Adsorption. The effect of nanoporous structures on protein adsorption was studied by using the nanoporous PEGDMA microparticles for adsorbing FITC-BSA (0.5 mg mL^{-1}) in aqueous solutions. The CLSM images of the microparticles before and after adsorption for 2 h were recorded by CLSM. Nonporous PEGDMA microparticles, the same size as that of the nanoporous microparticles, were used as the control group.

The BSA adsorption profile of the hierarchical porous microparticles was investigated by measuring the BSA concentration with a UV−vis spectrophotometer (UV-9600, Rayleigh) at 280 nm. Four samples, including nonporous PEGDMA microparticles, nanoporous PEGDMA microparticles, magnetic nanoporous poly(MMA-*co*-EGDMA-*co*-GMA) microparticles, and magnetic hierarchical porous poly(MMA-*co*-EGDMA-*co*-GMA) microparticles containing two micrometer-sized pores, were, respectively, used for the BSA adsorption. The nanoporous structures of the samples all resulted from addition of 10% (w/v) PGPR in the recipe. For the BSA adsorption, 0.5 g of microparticles was added into 5 mL of BSA solution (1.0 mg mL^{-1}), and kept still at room temperature for BSA adsorption. The time-dependent change in the absorbance of BSA solution was monitored by UV−vis spectrophotometer to estimate the change of BSA concentration in the solution. The adsorption amount (Q_m, mg g^{-1}) at t min can be calculated by the following equation

$$Q_m = (C_0 - C_t)V/m \tag{6}$$

where C_0 and C_t are the BSA concentration in solution at 0 min and t min, respectively; V is the volume of the BSA solution; and m is the mass quality of the microparticles.

RESULTS AND DISCUSSION

Strategy for Fabrication of Controllable Highly Interconnected Hierarchical Porous Microparticles. The fabrication procedure of the controllable highly interconnected hierarchical porous microparticles is schematically illustrated in Figure 1. Monodisperse water-in-oil-in-water (W/O/W) emulsions, with partially water-soluble organic monomer solution containing cross-linker and surfactant as oil phase, are generated from microfluidics for the microparticle fabrication (Figure 1a). The oil phase is partially miscible with the inner aqueous microdrop and outer aqueous continuous phase, leading to deformation of the emulsions into controllable shapes depending on the confined packing

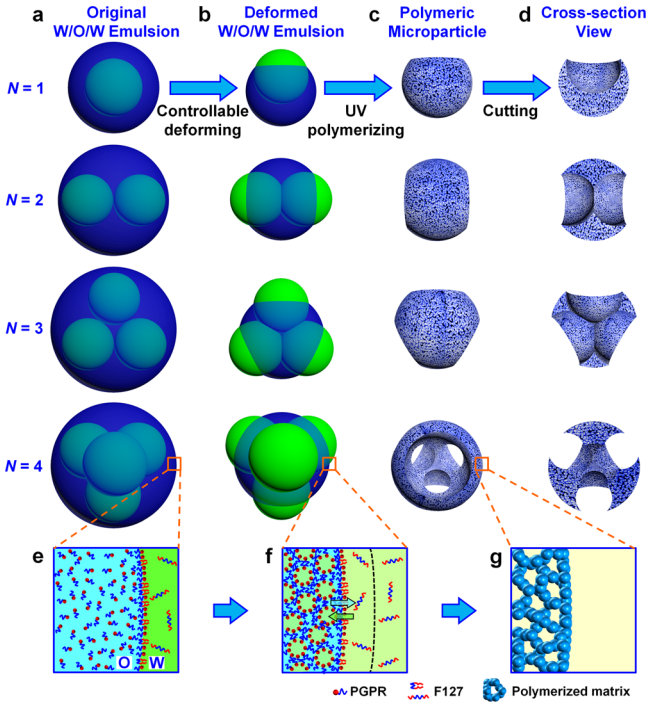

Figure 1. Strategy for controllable fabrication of highly interconnected hierarchical porous microparticles. (a−d) Fabrication of microparticles with controllable micrometer-sized pore structures and shapes from controllably deformed W/O/W emulsions containing an oil phase that is partially miscible with the aqueous phases. (e−g) Formation of nanoporous structures by employing mass-transfer-induced formation of aqueous nanodrops in oil phase as templates.

DOI: 10.1021/acsami.5b01031
ACS Appl. Mater. Interfaces 2015, 7, 13758−13767

structure of the inner microdrops (Figure 1a,b). This process also facilitates the mass-exchange between the oil phase and aqueous phase, leading to diffusion of water molecules into the oil phase to form aqueous nanodrops due to the presence of excess surfactant (Figure 1e,f). After UV-polymerization, micrometer-sized pores and nanometer-sized pores can be, respectively, templated from the inner microdrops and nanodrops to form uniform hierarchically engineered microparticles with highly interconnected hierarchical porous structures and controllable shapes (Figure 1c,d,g). For these hierarchical porous microparticles, the nanoporous structure of the polymeric matrix determines the specific surface area, while the micrometer-sized pores determine the shape of the nanoporous polymeric matrixes. The porosity of the micrometer-sized pores and nanometer-sized pores can be separately tuned by simply changing the size and number (N) of the inner drops and the amount of the surfactant in the oil phase. Meanwhile, these hierarchical porous microparticles can be flexibly functionalized by adding functional nanoparticles and monomers in the oil phase of the recipe in the fabrication. Thus, this approach allows controllable fabrication of uniform polymeric microparticles containing highly interconnected hierarchical porous structures, with pore size, porosity, functionality, and particle shape individually and flexibly manipulated in a single step. First, the fabrication approach is demonstrated by producing hierarchically engineered poly(MMA-*co*-EGDMA) microparticles with controllable hierarchical porous structures and shapes. Then, we demonstrate the flexible functionalization of our strategy by fabricating hierarchical porous poly(MMA-*co*-EGDMA) microparticles functionalized with magnetic nanoparticles for easy magnetic separation of oil from water. Moreover, magnetic hierarchical porous poly(MMA-*co*-EGDMA) microparticles modified with functional GMA are synthesized for enhanced protein adsorption.

Uniform Microparticles with Controllable Micrometer-Sized Pores and Tunable Shapes. Monodisperse W/O/W emulsions are generated from microfluidics as templates for synthesis of uniform hierarchical porous microparticles (Figure 2a). First, we focus on the fabrication of uniform microparticles with controllable micrometer-sized pores and tunable shapes. Typically, MMA containing cross-linker EGDMA, surfactant PGPR, and photoinitiator HMPP is used as oil fluid to form the middle oil layer of W/O/W emulsions. An aqueous solution containing glycerin and surfactant Pluronic F127 is used as inner and outer aqueous fluids to form, respectively, the inner microdrop and outer continuous phase. The high controllability of microfluidics allows precise control of the emulsion drop size,[49] and the inner drop number (N) (Figure 2b,c) by tuning flow rates. Thus, monodisperse W/O/W emulsions can be generated (Figure 3a), with controllable inner microdrops as templates to create porous structures with tunable size and porosity of micrometer-sized pores.

Due to the partially miscible property of the oil phase with the inner and outer aqueous phases, the W/O/W emulsions containing inner microdrops with controlled numbers can controllably deform into desired shapes depending on the confined packing structure of the inner microdrops (Figure 3a,b). It is worth noting that the deformation process can lead to partial dewetting of the oil phase on the inner microdrops, resulting in a thin film consisting of surfactant bilayers between the inner aqueous microdrop and outer aqueous phase (Figure 3c). Meanwhile, this deformation process also squeezes the inner microdrops together, forming a thin oil film between the inner and outer aqueous phases. The thin films could rupture after polymerizing the emulsion templates; thus, they are crucial for creating highly interconnected open micrometer-sized pores. Besides the packing microdrop structure, the processing time also influences the emulsion structures such as the shell thickness and shapes, which are dependent on the inner microdrop number (Figure 3d,e). For example, for W/O/W emulsions containing one microdrop, after processing for 6 min, the emulsions remain spherical, but the oil shell thickness decreases from tens of microns to several microns (Figure 3d). For W/O/W emulsions containing two microdrops, the emulsion shape changes from sphere into ellipsoid with the time going (Figure 3e). Thus, combination of the controllable inner microdrops and the processing time allows good control of the emulsion structure as well as the resultant microparticle shape and the micrometer-sized pore structure (Supporting Information Figure S1). After UV-polymerization of the controllably deformed emulsions containing inner microdrops with tunable numbers, uniform microparticles with controllable shapes and highly interconnected micrometer-sized open pores can be produced (Figure 4).

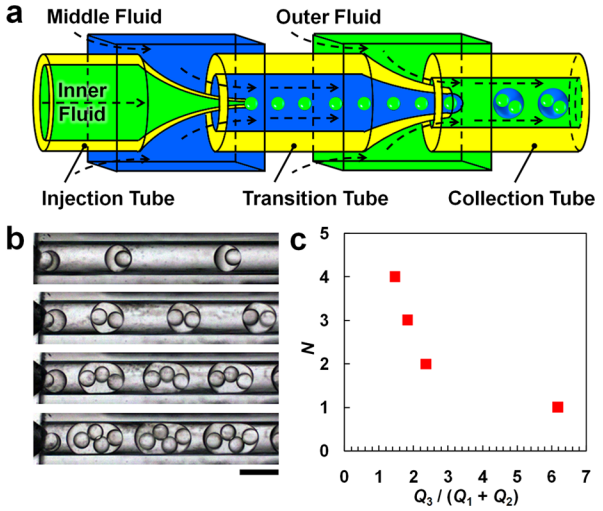

Figure 2. Microfluidic production of controllable W/O/W emulsion templates. (a,b) Microfluidic device for generating monodisperse controllable W/O/W emulsions, with high-speed optical micrographs showing their generation process (b). (c) Effect of flow rates on the number (N) of inner microdrops in the W/O/W emulsions. The flow rates of the inner fluid (Q_1) and middle fluid (Q_2) are 400 and 1000 μL h^{-1}, respectively. The flow rate of the outer fluid (Q_3) is adjusted to tune the N values. Scale bar is 400 μm.

Uniform Microparticles with Controllable Highly Interconnected Hierarchical Porous Structures. Integration of controllable nanometer-sized pores in the microparticles containing micrometer-sized pores is achieved by using mass-transfer-induced formation of aqueous nanodrops in the oil shell of W/O/W emulsions as templates. During the emulsion deformation, the partially miscible property of the oil phase with the aqueous phase facilitates the mass-exchange between the oil and aqueous phases. Thus, water molecules diffuse into the oil shell to form aqueous nanodrops, which can be stabilized by the excess amount of surfactant PGPR in the oil phase. We confirm this nanodrop formation by adding EGDMA microdrops containing 10% (w/v) PGPR into the continuous aqueous phase (Figure 5a). Fluorescent Rhodamine

DOI: 10.1021/acsami.5b01031
ACS Appl. Mater. Interfaces 2015, 7, 13758−13767

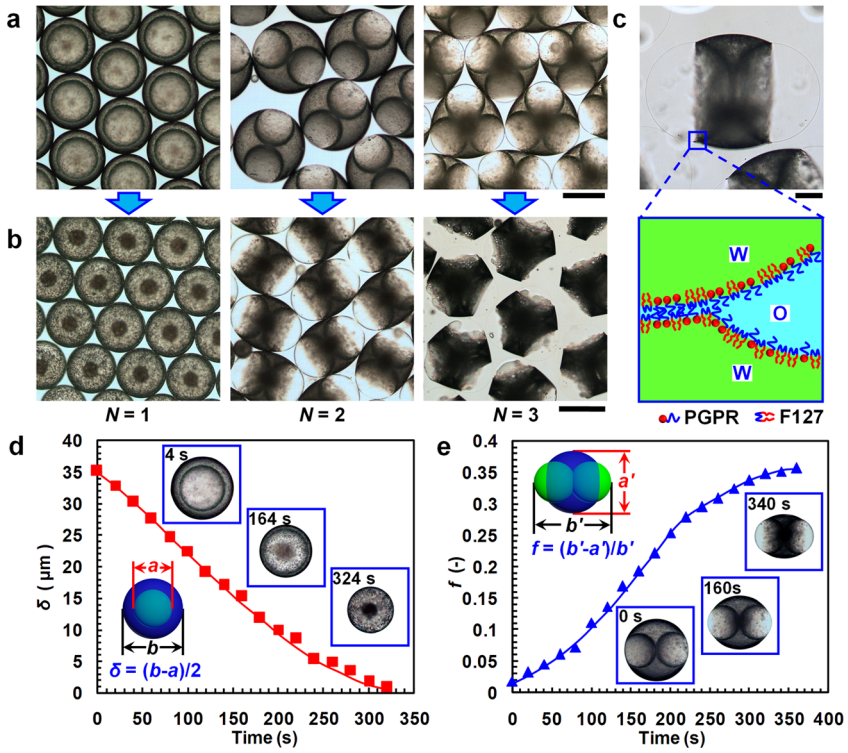

Figure 3. Controllable deformation of W/O/W emulsion templates. (a, b) Optical micrographs showing W/O/W emulsions containing microdrops with tunable number (N) before (a) and after (b) controllable deformation. (c) Optical micrograph of a deformed W/O/W emulsion containing two microdrops, with oil shell partially dewetting on the inner microdrop to form a surfactant bilayer. (d,e) Time-dependent change in the shell thickness (δ) of W/O/W emulsions containing one microdrop (d), and in the ellipticity (f) of W/O/W emulsions containing two microdrops (e). Scale bars are 200 μm in parts a and b, and 50 μm in part c.

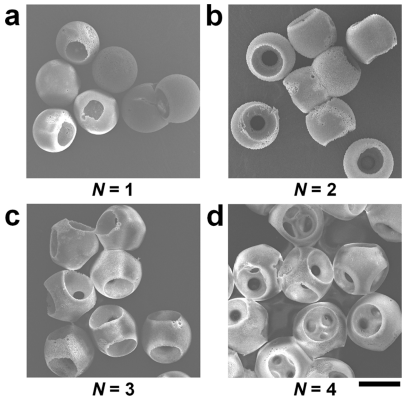

Figure 4. SEM images of poly(MMA-*co*-EGDMA) microparticles with tunable number (N = 1−4) of highly interconnected micrometer-sized pores and controllable shapes. Scale bar is 200 μm.

B is added in the aqueous phase to allow confocal laser scanning microscope (CLSM) to trace the diffusion of water molecules into the microdrops. With increasing processing time, red aqueous nanodrops with increasing numbers are observed inside the EGDMA microdrop, resulting in an increased fluorescent intensity. Since the mass-exchange-induced nanodrop formation is mainly due to the presence of excess surfactant PGPR, change of the surfactant amount in the oil phase allows adjustment of the nanodrop formation; thus, the nanoporosity can be tuned. For example, the nanoporosity of PEGDMA microparticles that is synthesized from EGDMA microdrops increases from 0% to 49.4% with an increasing amount of surfactant PGPR from 0% (w/v) to 50% (w/v) (Figure 5b). With an increase in the PGPR amount, the mechanical strength of the PEGDMA microparticle decreases due to the increased porosity (Figure 5b and Supporting Information Figure S2). As observed in the SEM images (Figure 6), the PEGDMA microparticles with 0% (w/v) PGPR show nonporous structures (Figure 6a) due to the absence of nanodrops in the oil phase, while the PEGDMA microparticles prepared from EGDMA drops with 10% (w/v) PGPR content (Figure 5a) exhibit highly interconnected nanoporous structures (Figure 6e). It is worth noting that, by gradually increasing the PGPR content from 0% to 10% (w/v), the PEGDMA microparticles exhibit a structure transition from a nonporous structure (Figure 6a), to an isolated porous structure (Figure 6b), to a highly interconnected porous structure (Figure 6c−e), depending on the PGPR content as well as the fraction of aqueous nanodrops in the oil phase. Moreover, by further increasing the PGPR content from 10% to 50% (w/v), microparticles with highly interconnected porous structures of increased porosity can be obtained (Figures 6f and 5b). As a typical example, the average pore size of the nanoporous PEGDMA microparticles prepared with 10% (w/v) PGPR is ∼180 nm (insert in Figure 5b), as measured by mercury intrusion porosimetry. The N_2 adsorption isotherms of the nanoporous microparticles also indicate the pore sizes fall in the "macroporous" (pore size >50 nm) category based on the IUPAC definition (Supporting Information Figure S3).[50]

An elaborate combination of the highly interconnected nanometer-sized pore structures and the micrometer-sized pore structures enables fabrication of highly interconnected hierarchical porous microparticles (Figure 7). The SEM images of the hierarchical porous poly(MMA-*co*-EGDMA) microparticles

DOI: 10.1021/acsami.5b01031
ACS Appl. Mater. Interfaces 2015, 7, 13758−13767

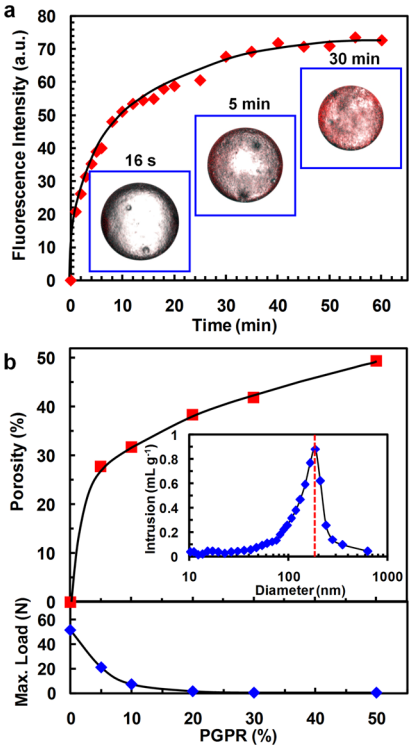

Figure 5. Mass-transfer-induced creation of nanoporous structures. (a) Time-dependent change in the fluorescent intensity of EGDMA drops with 10% (w/v) PGPR in aqueous phase. (b) Porosity and the mechanical strength of PEGDMA microparticles fabricated with different amounts of PGPR, with the inset showing the size distribution of the nanometer-sized pores of PEGDMA microparticles with 10% (w/v) PGPR measured by mercury intrusion porosimetry. The "Max. Load" in the *y*-axis presents the maximum load at fracture upon compression, and the values are obtained from the compressive load−strain curves shown in Supporting Information Figure S2.

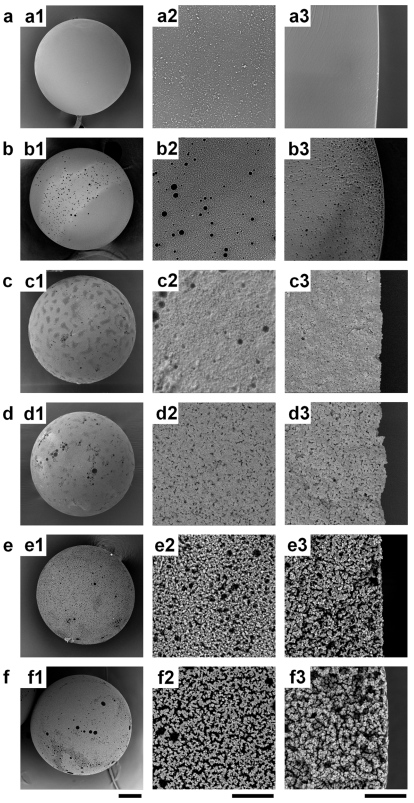

Figure 6. SEM images of PEGDMA microparticles with 0% (a1), 5% (b1), 7% (c1), 9% (d1), 10% (e1), and 50% (f1) PGPR, and their outer surfaces (a2−f2) and cross sections (a3−f3). Scale bars are 50 μm in a1−f1, and 20 μm in the rest.

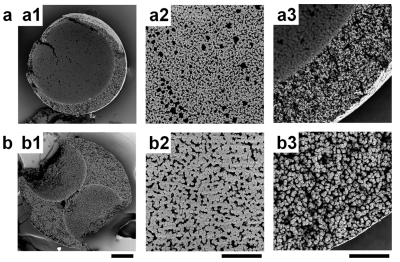

Figure 7. Integration of controllable nanometer-sized pore structures and micrometer-sized pore structures for fabricating hierarchical porous microparticles. SEM images of ruptured hierarchical porous poly(MMA-*co*-EGDMA) microparticles with one micrometer-sized pore (a1) and magnetic hierarchical porous poly(MMA-*co*-EGDMA-*co*-GMA) microparticles with two micrometer-sized pores (b1), as well as their magnified outer surfaces (a2−b2) and cross sections (a3−b3). Scale bars are 50 μm in a1−b1, and 20 μm in the rest.

clearly show the single micrometer-sized pore in the microparticle, and the highly interconnected nanoporous structures on the outer surface and the cross-section (Figure 7a). The emulsion-templated synthesis process of the hierarchical porous microparticles enables flexible functionalization of the microparticles by incorporating functional components into the oil phase. We demonstrate this advantage by adding GMA and magnetic nanoparticles (Supporting Information Figure S4) in the oil phase to produce magnetic hierarchical porous poly(MMA-*co*-EGDMA-*co*-GMA) containing two micrometer-sized pores (Figure 7b). This fabrication approach enables formation of controllable highly interconnected porous microparticles with both micrometer-sized pores and nanometer-sized pores, tunable particle shapes, and flexible functionalities in a single step, thus providing a facile and versatile strategy for fabricating functional hierarchical porous microparticles.

Removal of Oil Drops from Water for Purification. The hierarchical porous poly(MMA-*co*-EGDMA) microparticles provide hydrophobic porous matrix carriers for adsorption of oil drops from water. For microparticles with only nanoporous structure, the hydrophobic surface of the nanometer-sized pores allows wetting of oil drop on the nanoporous matrixes for oil loading, while the nanoporosity determines the loading capacity (Figure 8a). With integration of micrometer-sized pores in the nanoporous matrixes, the micrometer-sized pores can serve as microcontainers to provide improved spaces in the microparticles for oil loading, thus leading to larger capacity for capturing oil (Figure 8b). Upon further incorporation of the hierarchical porous matrix with magnetic nanoparticles, the microparticles can be used to remove oil drops from water via magnetic manipulation, as demonstrated in Figure 8c. EGDMA dyed with LR300 (red color) is used as sample oil, and is added into water (Figure 8c1) and then shaken into microdrops (Figure 8c2). Then, magnetic poly(MMA-*co*-EGDMA) microparticles with hierarchical porous structures containing three micrometer-sized pores are added (Figure 8c3), and are mixed with the EGDMA microdrops by shaking for oil adsorption. After that, the oil-adsorbed microparticles can be easily separated by a magnet for oil removal (Figure 8c4), and can

DOI: 10.1021/acsami.5b01031
ACS Appl. Mater. Interfaces 2015, 7, 13758−13767

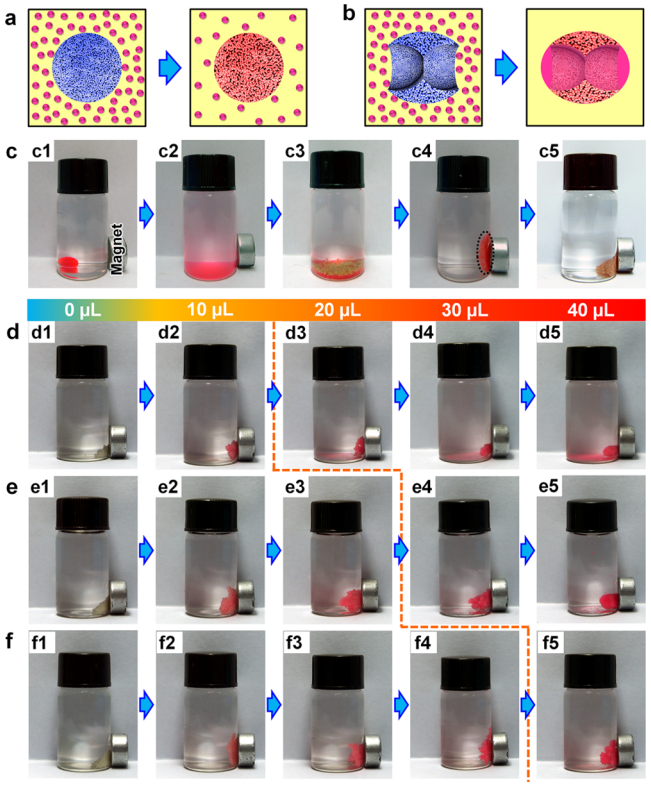

Figure 8. Hierarchical porous microparticles for oil removal. (a, b) Schematic illustration of oil capture with nanoporous (a) and hierarchical porous (b) microparticles. (c) Magnetic hierarchical porous poly(MMA-*co*-EGDMA) microparticles for magnetic-guided removal of EGDMA microdrops from water. A large EGDMA drop (c1) is shaken into microdrops (c2), and then microparticles are added (c3); next, the oil-adsorbed microparticles are separated by a magnet (c4), and then washed with ethanol for recycle (c5). (d–f) Nanoporous (d) and hierarchical porous poly(MMA-*co*-EGDMA-*co*-GMA) microparticles with two (e) and three (f) micrometer-sized pores for quantitative oil removal.

be further recycled by washing off the adsorbed oil with ethanol for reuse (Figure 8c5). In the experiments, the magnetic microparticles can be recycled more than 20 times. Moreover, washing and immersing the microparticles with ethanol makes no obvious change to the porous structures (Figure 7a and Supporting Information Figure S5). These hierarchical porous microparticles can also be employed for magnetic-guided removal of other oil that can spread on the porous matrix, such as benzyl benzoate (Supporting Information Figure S6). Moreover, on the basis of the magnetic-guided movement, the microparticles can also be used for route-specific targeted adsorption of oil microdrops (Supporting Information Figure S7).

Here the magnetic-guided removal of EGDMA oil drops by hierarchical porous poly(MMA-*co*-EGDMA-*co*-GMA) microparticles is also demonstrated, and the effects of the nanometer-sized pores, micrometer-sized pores, and hierarchical porous structures on the oil capturing capacity are quantitatively investigated (Figure 8d–f and Supporting Information Figure S8). For poly(MMA-*co*-EGDMA-*co*-GMA) microparticles containing only one micrometer-sized pore, with average pore size of ∼120 μm and porosity of 44.1%, oil drop leftovers are observed upon total addition of ∼10 μL oil drops (Supporting Information Figure S8a), indicating a maximum oil capturing capacity less than ∼10 μL. Such an oil capturing capacity is less than that of the poly(MMA-*co*-EGDMA-*co*-GMA) microparticles containing only nanometer-sized pores, with average pore size of ∼580 nm (Supporting Information Figure S9) and porosity of 47.7% (Supporting Information Figure S8b) (please see Supporting Information Table S1 for the pore characteristics of micrometer-sized pores and nanometer-sized pores of the hierarchical porous microparticles). The results show that nanometer-sized pores exhibit better performance for oil capture than the micrometer-sized pore, because the nanometer-sized pores provide a nanoporous matrix with a hydrophobic surface for wetting of oil via capillary force. Moreover, by gradually adding the oil drops, the nanoporous poly(MMA-*co*-EGDMA-*co*-GMA) microparticles (Figure 8d) exhibit maximum oil capture upon total addition of ∼20 μL oil drops (Figure 8d3), while those with hierarchical porous structures containing two (Figure 8e) and three (Figure 8f) micrometer-sized pores, respectively, exhibit the maximum oil capture at total addition of ∼30 μL (Figure 8e4) and ∼40 μL (Figure 8f5) oil drops. All the results show that the hierarchical porous poly(MMA-*co*-EGDMA-*co*-GMA) microparticles can capture a larger amount of oil than the nanoporous ones, and the maximum capacity for oil capture increases with increasing the number of micrometer-sized pores. Thus, as compared with the homogeneous nanoporous structures, the hierarchical porous structures provide opportunities for creating microparticles with larger oil capturing capacity from the same mass quality of matrix materials.

Enhanced Protein Adsorption. The enhanced synergetic performance of the hierarchical porous microparticles is demonstrated by using the microparticles for improved protein adsorption. As compared with nanoporous microparticles (Figure 9a1), the hierarchical porous microparticles provide highly interconnected micrometer-sized pores as easier access for the protein molecules to diffuse into the porous matrix (Figure 9a2). Meanwhile, the presence of the micrometer-sized pores also provides the nanoporous matrix with larger interfacial area between the microparticle and the BSA bulk solution, including the outer surface of the microparticle and the internal surface of the micrometer-sized pores, for the protein molecules to diffuse into the nanoporous matrix. Thus, faster adsorption of protein can be achieved with the hierarchical porous microparticles.

First, we demonstrate the protein adsorption performance of nanoporous microparticles by using nanoporous PEGDMA microparticles to adsorb model protein FITC-BSA. After immersion in FITC-BSA solution for 2 h, a large quantity of FITC-BSA is adsorbed within the nanoporous PEGDMA microparticles, while nearly no FITC-BSA is adsorbed within the nonporous PEGDMA ones (Supporting Information Figure S10). After transfer into water, the distribution of adsorbed FITC-BSA over the whole internal portion of nanoporous PEGDMA microparticles further confirms the adsorption ability and the high interconnectivity of the nanoporous structures (Supporting Information Figure S10).

The BSA adsorption is further quantitatively investigated to study the enhanced synergetic performance of hierarchical porous structures on the adsorption kinetics. Four different types of microparticles, including nonporous PEGDMA microparticles, nanoporous PEGDMA microparticles, magnetic nanoporous poly(MMA-*co*-EGDMA-*co*-GMA) microparticles, and magnetic hierarchical porous poly(MMA-*co*-EGDMA-*co*-GMA) microparticles containing two micrometer-sized pores,

DOI: 10.1021/acsami.5b01031
ACS Appl. Mater. Interfaces 2015, 7, 13758–13767

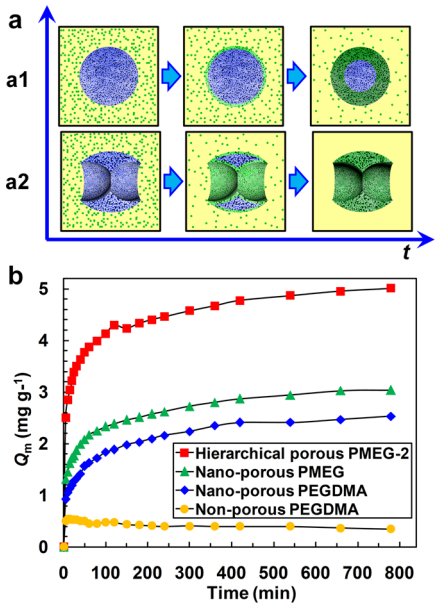

Figure 9. Hierarchical porous microparticles for protein adsorption. (a) Schematic illustration of dynamic processes of protein adsorption with nanoporous (a1) and hierarchical porous (a2) microparticles. (b) BSA adsorption profiles of nonporous PEGDMA microparticles, nanoporous PEGDMA microparticles, magnetic nanoporous poly(MMA-*co*-EGDMA-*co*-GMA) microparticles (PMEG), and magnetic hierarchical porous poly(MMA-*co*-EGDMA-*co*-GMA) microparticles with two micrometer-sized pores (PMEG-2).

are respectively employed. The microparticles are still immersed in BSA solutions to allow free diffusion of the BSA molecules. Due to the highly interconnected nanoporous structures for adsorbing BSA molecules, the nanoporous PEGDMA microparticles with specific surface area of 16.37 m^2 g^{-1} show a faster adsorption rate with higher adsorption capacity than the nonporous PEGDMA microparticles (Figure 9b). Improved BSA adsorption can be achieved by using magnetic nanoporous poly(MMA-*co*-EGDMA-*co*-GMA) microparticles with specific surface area of 16.83 m^2 g^{-1} as adsorbents (Figure 9b), because the nanoporous structures with GMA-modified interfaces provide better interactions with BSA molecules for enhanced adsorption. The presence of magnetic nanoparticles in the microparticles facilitates the separation via magnetic manipulation. The adsorption of such functional nanoporous poly(MMA-*co*-EGDMA-*co*-GMA) microparticles can be further improved by creating highly interconnected micrometer-sized pores in the microparticles for enhanced mass transfer kinetics. With hierarchical porous structures, hierarchical porous poly(MMA-*co*-EGDMA-*co*-GMA) microparticles containing two micrometer-sized pores exhibit a much faster adsorption rate (3.88 mg g^{-1} at t = 60 min) than those of the nanoporous poly(MMA-*co*-EGDMA-*co*-GMA) ones with only nanoporous structures (2.17 mg g^{-1} at t = 60 min) (Figure 9b).

Since the poly(MMA-*co*-EGDMA-*co*-GMA) microparticles containing nanoporous and hierarchical porous structures with the same total mass quality are used as adsorbents, and their polymeric matrixes are both prepared from oil phase with the same composition, therefore both types of microparticles exhibit polymeric matrixes with the same nanoporous structures and the same total mass quality. Thus, both types of these poly(MMA-*co*-EGDMA-*co*-GMA) microparticles exhibit the same specific surface areas, that are provided by the nanoporous polymeric matrixes, for maximum BSA adsorption. Therefore, the faster adsorption of the hierarchical porous poly(MMA-*co*-EGDMA-*co*-GMA) microparticles containing two micrometer-sized pores mainly results from the highly interconnected micrometer-sized pores. As compared with nanoporous microparticles, hierarchical porous microparticles with such micrometer-sized pore structures provide the nanoporous matrix with larger interfacial area between the microparticle and BSA bulk solution, including the outer surface of microparticle and the internal surface of micrometer-sized pores, for BSA to diffuse easily from bulk solution into the nanoporous matrix (Supporting Information Figure S11). Since the diffusion rate of BSA from bulk solution into the nanoporous matrix is the same, increase of the interfacial area of the microparticle that is exposed to the BSA bulk solution allows improved mass transfer of BSA from bulk solution into the nanoporous matrix for faster adsorption. Thus, for microparticles containing nanoporous matrixes with the same total mass quality, the more micrometer-sized pores created in the nanoporous matrix, the larger the interfacial area of the nanoporous matrix exposed to the BSA bulk solution (Supporting Information Figure S11); as a result, we can infer that this provides faster BSA adsorption. All the results indicate that the functional hierarchical porous microparticles with combined advantages of enhanced mass-transfer kinetics and flexibly tunable functionalities show great potential for enhanced protein adsorption.

CONCLUSIONS

In summary, we have developed a facile and flexible approach for one-step fabrication of uniform controllable polymeric microparticles containing highly interconnected hierarchical porous structures. The controllably deformed W/O/W emulsions, which are generated from microfluidics, enable production of uniform hierarchical porous microparticles with precisely and individually controlled pore size, porosity, functionality, and particle shape by using the inner microdrops and the nanodrops as templates for creating micrometer-sized pores and nanometer-sized pores, respectively. The hierarchical porous microparticles with controllable physical structures and chemical properties combine the advantages of porous structures at both micro- and nanoscales as well as the tunable functionalities to achieve enhanced synergetic performances for broad applications. The enhanced synergetic performances are demonstrated by using them to capture oil from water and adsorb protein molecules for bioseparation. The proposed approach provides a versatile strategy for controllable fabrication of uniform polymeric microparticles with highly interconnected hierarchical porous structures and tunable functionalities.

ASSOCIATED CONTENT

Supporting Information

Optical micrographs of the hierarchical porous microparticles, compressive load−strain curves and N_2 adsorption isotherms of nanoporous microparticles, TEM image of the magnetic nanoparticles, SEM images of hierarchical porous microparticles after ethanol washing, magnetic-guided removal of benzyl benzoate, magnetic-guided route-specific adsorption of oil microdrops, pore size distribution of nanoporous poly(MMA-*co*-EDGMA-*co*-GMA) microparticles, CLSM images of microparticles for FITC-BSA adsorption, interfacial area data, and a table that summarizes pore characteristics of hierarchical

DOI: 10.1021/acsami.5b01031
ACS Appl. Mater. Interfaces 2015, 7, 13758−13767

porous microparticles. The Supporting Information is available free of charge on the ACS Publications website at DOI: 10.1021/acsami.5b01031.

AUTHOR INFORMATION

Corresponding Authors

*E-mail: wangwei512@scu.edu.cn.
*E-mail: chuly@scu.edu.cn.

Author Contributions

The manuscript was written through contributions of all authors. All authors have given approval to the final version of the manuscript.

Notes

The authors declare no competing financial interest.

ACKNOWLEDGMENTS

The authors gratefully acknowledge support from the National Natural Science Foundation of China (91434202, 21322605), the Program for Changjiang Scholars and Innovative Research Team in University (IRT1163), and State Key Laboratory of Polymer Materials Engineering (sklpme2014-1-01). We thank Ms. X.-Y. Zhang in the Analytical and Testing Center of Sichuan University for her help in the SEM imaging.

REFERENCES

(1) Parlett, C. M. A.; Wilson, K.; Lee, A. F. Hierarchical Porous Materials: Catalytic Applications. *Chem. Soc. Rev.* **2013**, *42*, 3876–3893.

(2) Li, Y.; Fu, Z. Y.; Su, B. L. Hierarchically Structured Porous Materials for Energy Conversion and Storage. *Adv. Funct. Mater.* **2012**, *22*, 4634–4667.

(3) Yuan, Z. Y.; Su, B. L. Insights into Hierarchically Meso-Macroporous Structured Materials. *J. Mater. Chem.* **2006**, *16*, 663–677.

(4) Yu, H.; Qiu, X.; Nunes, S. P.; Peinemann, K. V. Biomimetic Block Copolymer Particles with Gated Nanopores and Ultrahigh Protein Sorption Capacity. *Nat. Commun.* **2014**, *5*, 4110.

(5) Abbaspourrad, A.; Carroll, N. J.; Kim, S. H.; Weitz, D. A. Surface Functionalized Hydrophobic Porous Particles Toward Water Treatment Application. *Adv. Mater.* **2013**, *25*, 3215–3221.

(6) Liu, X. H.; Jin, X. B.; Ma, P. X. Nanofibrous Hollow Microspheres Self-Assembled from Star-Shaped Polymers as Injectable Cell Carriers for Knee Repair. *Nat. Mater.* **2011**, *10*, 398–406.

(7) Edwards, D. A.; Hanes, J.; Caponetti, G.; Hrkach, J.; BenJebria, A.; Eskew, M. L.; Mintzes, J.; Deaver, D.; Lotan, N.; Langer, R. Large Porous Particles for Pulmonary Drug Delivery. *Science* **1997**, *276*, 1868–1871.

(8) Chung, H. J.; Park, T. G. Surface Engineered and Drug Releasing Pre-Fabricated Scaffolds for Tissue Engineering. *Adv. Drug Delivery Rev.* **2007**, *59*, 249–262.

(9) Nakayama, D.; Takeoka, Y.; Watanabe, M.; Kataoka, K. Simple and Precise Preparation of a Porous Gel for a Colorimetric Glucose Sensor by a Templating Technique. *Angew. Chem., Int. Ed.* **2003**, *42*, 4197–4200.

(10) Zhao, X. W.; Cao, Y.; Ito, F.; Chen, H. H.; Nagai, K.; Zhao, Y. H.; Gu, Z. Z. Colloidal Crystal Beads as Supports for Biomolecular Screening. *Angew. Chem., Int. Ed.* **2006**, *45*, 6835–6838.

(11) Qu, J. B.; Wan, X. Z.; Zhai, Y. Q.; Zhou, W. Q.; Su, Z. G.; Ma, G. H. A Novel Stationary Phase Derivatized from Hydrophilic Gigaporous Polystyrene-Based Microspheres for High-Speed Protein Chromatography. *J. Chromatogr. A* **2009**, *1216*, 6511–6516.

(12) Sacanna, S.; Irvine, W. T. M.; Chaikin, P. M.; Pine, D. J. Lock and Key Colloids. *Nature* **2010**, *464*, 575–578.

(13) Damasceno, P. F.; Engel, M.; Glotzer, S. C. Predictive Self-Assembly of Polyhedra into Complex Structures. *Science* **2012**, *337*, 453–457.

(14) De La Vega, J. C.; Elischer, P.; Schneider, T.; Hafeli, U. O. Uniform Polymer Microspheres: Monodispersity Criteria, Methods of Formation and Applications. *Nanomedicine* **2013**, *8*, 265–285.

(15) Xu, Q.; Hashimoto, M.; Dang, T. T.; Hoare, T.; Kohane, D. S.; Whitesides, G. M.; Langer, R.; Anderson, D. G. Preparation of Monodisperse Biodegradable Polymer Microparticles Using a Microfluidic Flow-Focusing Device for Controlled Drug Delivery. *Small* **2009**, *5*, 1575–1581.

(16) Weitz, D. A. Packing in the Spheres. *Science* **2004**, *303*, 968–969.

(17) Donev, A.; Cisse, I.; Sachs, D.; Variano, E.; Stillinger, F. H.; Connelly, R.; Torquato, S.; Chaikin, P. M. Improving the Density of Jammed Disordered Packings using Ellipsoids. *Science* **2004**, *303*, 990–993.

(18) John, U.; Lennart, S.; Arvid, B.; Jan, B. Monodisperse Polymer Particles - A Step Forward for Chromatography. *Nature* **1983**, *303*, 95–96.

(19) Gokmen, M. T.; Du Prez, F. E. Porous Polymer Particles-A Comprehensive Guide to Synthesis, Characterization, Functionalization and Applications. *Prog. Polym. Sci.* **2012**, *37*, 365–405.

(20) Lu, Y. F.; Fan, H. Y.; Stump, A.; Ward, T. L.; Rieker, T.; Brinker, C. J. Aerosol-Assisted Self-Assembly of Mesostructured Spherical Nanoparticles. *Nature* **1999**, *398*, 223–226.

(21) Kresge, C. T.; Leonowicz, M. E.; Roth, W. J.; Vartuli, J. C.; Beck, J. S. Ordered Mesoporous Molecular Sieves Synthesized by a Liquid-Crystal Template Mechanism. *Nature* **1992**, *359*, 710–712.

(22) Zhao, D. Y.; Feng, J. L.; Huo, Q. S.; Melosh, N.; Fredrickson, G. H.; Chmelka, B. F.; Stucky, G. D. Triblock Copolymer Syntheses of Mesoporous Silica with Periodic 50 to 300 Angstrom Pores. *Science* **1998**, *279*, 548–552.

(23) Warren, S. C.; Messina, L. C.; Slaughter, L. S.; Kamperman, M.; Zhou, Q.; Gruner, S. M.; DiSalvo, F. J.; Wiesner, U. Ordered Mesoporous Materials from Metal Nanoparticle-Block Copolymer Self-Assembly. *Science* **2008**, *320*, 1748–1752.

(24) Yang, P. D.; Zhao, D. Y.; Margolese, D. I.; Chmelka, B. F.; Stucky, G. D. Generalized Syntheses of Large-Pore Mesoporous Metal Oxides with Semicrystalline Frameworks. *Nature* **1998**, *396*, 152–155.

(25) Dinsmore, A. D.; Hsu, M. F.; Nikolaides, M. G.; Marquez, M.; Bausch, A. R.; Weitz, D. A. Colloidosomes: Selectively Permeable Capsules Composed of Colloidal Particles. *Science* **2002**, *298*, 1006–1009.

(26) Velev, O. D.; Lenhoff, A. M.; Kaler, E. W. A Class of Microstructured Particles through Colloidal Crystallization. *Science* **2000**, *287*, 2240–2243.

(27) Zakhidov, A. A.; Baughman, R. H.; Iqbal, Z.; Cui, C. X.; Khayrullin, I.; Dantas, S. O.; Marti, I.; Ralchenko, V. G. Carbon Structures with Three-Dimensional Periodicity at Optical Wavelengths. *Science* **1998**, *282*, 897–901.

(28) Velev, O. D.; Jede, T. A.; Lobo, R. F.; Lenhoff, A. M. Porous Silica via Colloidal Crystallization. *Nature* **1997**, *389*, 447–448.

(29) Holland, B. T.; Blanford, C. F.; Stein, A. Synthesis of Macroporous Minerals with Highly Ordered Three-Dimensional Arrays of Spheroidal Voids. *Science* **1998**, *281*, 538–540.

(30) Imhof, A.; Pine, D. J. Ordered Macroporous Materials by Emulsion Templating. *Nature* **1997**, *389*, 948–951.

(31) Imhof, A.; Pine, D. J. Uniform Macroporous Ceramics and Plastics by Emulsion Templating. *Adv. Mater.* **1998**, *10*, 697–700.

(32) Kim, T. K.; Yoon, J. J.; Lee, D. S.; Park, T. G. Gas Foamed Open Porous Biodegradable Polymeric Microspheres. *Biomaterials* **2006**, *27*, 152–159.

(33) Nakanishi, K.; Tanaka, N. Sol-Gel with Phase Separation. Hierarchically Porous Materials Optimized for High-Performance Liquid Chromatography Separations. *Acc. Chem. Res.* **2007**, *40*, 863–873.

(34) Davis, S. A.; Burkett, S. L.; Mendelson, N. H.; Mann, S. Bacterial Templating of Ordered Macrostructures in Silica and Silica-Surfactant Mesophases. *Nature* **1997**, *385*, 420–423.

(35) Sai, H.; Tan, K. W.; Hur, K.; Asenath-Smith, E.; Hovden, R.; Jiang, Y.; Riccio, M.; Muller, D. A.; Elser, V.; Estroff, L. A.; Gruner, S.

DOI: 10.1021/acsami.5b01031
ACS Appl. Mater. Interfaces 2015, 7, 13758–13767

M.; Wiesner, U. Hierarchical Porous Polymer Scaffolds from Block Copolymers. *Science* **2013**, *341*, 530−534.
(36) Stein, A.; Li, F.; Denny, N. R. Morphological Control in Colloidal Crystal Templating of Inverse Opals, Hierarchical Structures, and Shaped Particles. *Chem. Mater.* **2008**, *20*, 649−666.
(37) Fan, J. B.; Huang, C.; Jiang, L.; Wang, S. Nanoporous Microspheres: From Controllable Synthesis to Healthcare Applications. *J. Mater. Chem. B* **2013**, *1*, 2222−2235.
(38) Wu, D.; Xu, F.; Sun, B.; Fu, R.; He, H.; Matyjaszewski, K. Design and Preparation of Porous Polymers. *Chem. Rev.* **2012**, *112*, 3959−4015.
(39) Yang, P. D.; Deng, T.; Zhao, D. Y.; Feng, P. Y.; Pine, D.; Chmelka, B. F.; Whitesides, G. M.; Stucky, G. D. Hierarchically Ordered Oxides. *Science* **1998**, *282*, 2244−2246.
(40) Atencia, J.; Beebe, D. J. Controlled Microfluidic Interfaces. *Nature* **2005**, *437*, 648−655.
(41) Wang, W.; Zhang, M. J.; Chu, L. Y. Functional Polymeric Microparticles Engineered from Controllable Microfluidic Emulsions. *Acc. Chem. Res.* **2014**, *47*, 373−384.
(42) Xu, S. Q.; Nie, Z. H.; Seo, M.; Lewis, P.; Kumacheva, E.; Stone, H. A.; Garstecki, P.; Weibel, D. B.; Gitlin, I.; Whitesides, G. M. Generation of Monodisperse Particles by using Microfluidics: Control over Size, Shape, and Composition. *Angew. Chem., Int. Ed.* **2005**, *44*, 724−728.
(43) Wang, W.; Zhang, M. J.; Xie, R.; Ju, X. J.; Yang, C.; Mou, C. L.; Weitz, D. A.; Chu, L. Y. Hole-Shell Microparticles from Controllably Evolved Double Emulsions. *Angew. Chem., Int. Ed.* **2013**, *52*, 8084−8087.
(44) Choi, S.-W.; Zhang, Y.; Xia, Y. Fabrication of Microbeads with a Controllable Hollow Interior and Porous Wall Using a Capillary Fluidic Device. *Adv. Funct. Mater.* **2009**, *19*, 2943−2949.
(45) Wan, J.; Bick, A.; Sullivan, M.; Stone, H. A. Controllable Microfluidic Production of Microbubbles in Water-in-Oil Emulsions and the Formation of Porous Microparticles. *Adv. Mater.* **2008**, *20*, 3314−3318.
(46) Zhang, J.; Coulston, R. J.; Jones, S. T.; Geng, J.; Scherman, O. A.; Abell, C. One-Step Fabrication of Supramolecular Microcapsules from Microfluidic Droplets. *Science* **2012**, *335*, 690−694.
(47) Lee, D.; Weitz, D. A. Nonspherical Colloidosomes with Multiple Compartments from Double Emulsions. *Small* **2009**, *5*, 1932−1935.
(48) Liu, Y.-M.; Wang, W.; Zheng, W.-C.; Ju, X.-J.; Xie, R.; Zerrouki, D.; Deng, N.-N.; Chu, L.-Y. Hydrogel-Based Microactuators with Remote-Controlled Locomotion and Fast Pb2+-Response for Micromanipulation. *ACS Appl. Mater. Interfaces* **2013**, *5*, 7219−7226.
(49) Chu, L. Y.; Utada, A. S.; Shah, R. K.; Kim, J. W.; Weitz, D. A. Controllable Monodisperse Multiple Emulsions. *Angew. Chem., Int. Ed.* **2007**, *46*, 8970−8974.
(50) Sing, K. S. W.; Everett, D. H.; Haul, R. A. W.; Moscou, L.; Pierotti, R. A.; Rouquérol, J.; Siemieniewska, T. Reporting Physisorption Data for Gas/Solid Systems with Special Reference to the Determination of Surface Area and Porosity. *Pure Appl. Chem.* **1985**, *57*, 603−619.

DOI: 10.1021/acsami.5b01031
ACS Appl. Mater. Interfaces 2015, 7, 13758−13767